

Comparing photonic band structure calculation methods for diamond and pyrochlore crystals

E. C. M. Vermolen,¹ J. H. J. Thijssen,^{1,2} A. Moroz,³ M. Megens,⁴ and A. van Blaaderen^{1*}

¹ *Soft Condensed Matter, Debye Institute for NanoMaterials Science, Utrecht University, Princetonplein 1, NL-3584 CC Utrecht, the Netherlands*

² *Present address: SUPA School of Physics and Astronomy, University of Edinburgh, Edinburgh, EH9 3JZ, United Kingdom*

³ <http://www.wave-scattering.com>

⁴ *Philips Research Laboratories, High Tech Campus 34, NL-5656 AE Eindhoven, the Netherlands*

[*A.vanBlaaderen@uu.nl](mailto:A.vanBlaaderen@uu.nl)

<http://www.colloid.nl>

Abstract: The photonic band diagrams of close-packed colloidal diamond and pyrochlore structures, have been studied using Korringa-Kohn-Rostoker (KKR) and plane-wave calculations. In addition, the occurrence of a band gap has been investigated for the binary Laves structures and their constituent large- and small-sphere substructures. It was recently shown that these Laves structures give the possibility to fabricate the diamond and pyrochlore structures by self-organization. The comparison of the two calculation methods opens the possibility to study the validity and the convergence of the results, which have been an issue for diamond-related structures in the past. The KKR calculations systematically give a lower value for the gap width than the plane-wave calculations. This difference can partly be ascribed to a convergence issue in the plane-wave code when a contact point of two spheres coincides with the grid.

© 2009 Optical Society of America

OCIS codes: (050.5298) Photonic crystals; (050.1755) Computational electromagnetic methods; (160.5293) Photonic bandgap materials; (160.5298) Photonic crystals

References and links

1. P. Lodahl, A. F. van Driel, I. S. Nikolaev, A. Irman, K. Overgaag, D. L. Vanmaekelbergh, and W. L. Vos, "Controlling the dynamics of spontaneous emission from quantum dots by photonic crystals," *Nature* **430**, 654–657 (2004).
2. V. P. Bykov, "Spontaneous emission in a periodic structure," *Soviet Physics - JETP* **35**, 269–273 (1972).
3. V. P. Bykov, "Spontaneous emission from a medium with a band spectrum," *Sov. J. Quantum Electron.* **4**, 861–871 (1975).
4. E. Yablonovitch, "Inhibited Spontaneous Emission in Solid-State Physics and Electronics," *Phys. Rev. Lett.* **58**, 2059–2062 (1987).
5. S. John, "Strong localization of photons in certain disordered dielectric superlattices," *Phys. Rev. Lett.* **58**, 2486–2489 (1987).
6. *Photonic Crystals and Light Localization in the 21st Century*, NATO Science Series (C): Mathematical and Physical Sciences (Kluwer Academic, Dordrecht, 2001).
7. K. Busch, S. Lölkes, R. B. Wehrspohn, and H. Föll (ed.), *Photonic Crystals: Advances in Design, Fabrication, and Characterization* (Wiley-VCH, Berlin, 2004).

8. K. Busch, G. von Freymann, S. Linden, S. Mingaleev, L. Tkeshelashvili, and M. Wegener, "Periodic nanostructures for photonics," *Phys. Rep.* **444**, 101–202 (2007).
9. K. M. Ho, C. T. Chan, and C. M. Soukoulis, "Existence of a photonic gap in periodic dielectric structures," *Phys. Rev. Lett.* **65**, 3152–3155 (1990).
10. M. Maldovan, C. K. Ullal, W. C. Carter, and E. L. Thomas, "Exploring for 3D photonic bandgap structures in the 11 f.c.c. space groups," *Nat. Mater.* **2**, 664–667 (2003).
11. A. Moroz, "Metallo-dielectric diamond and zinc-blende photonic crystals," *Phys. Rev. B* **66**, 115109 (2002).
12. A. J. Garcia-Adeva, "Band gap atlas for photonic crystals having the symmetry of the kagome and pyrochlore lattices," *New J. Phys.* **8**, 86 (2006).
13. T. T. Ngo, C. M. Liddell, M. Ghebrebrhan, and J. D. Joannopoulos, "Tetrastack: Colloidal diamond-inspired structure with omnidirectional photonic band gap for low refractive index contrast," *Appl. Phys. Lett.* **88**, 241920 (2006).
14. A. V. Tkachenko, "Morphological diversity of DNA-colloidal self-assembly," *Phys. Rev. Lett.* **89**, 148303 (2002).
15. F. García-Santamaría, H. T. Miyazaki, A. Urquía, M. Ibasate, M. Belmonte, N. Shinya, F. Meseguer, and C. López, "Nanorobotic Manipulation of Microspheres for On-Chip Diamond Architectures," *Adv. Mater.* **14**, 1144–1147 (2002).
16. M. Deubel, G. von Freymann, M. Wegener, S. Pereira, K. Busch, and C. M. Soukoulis, "Direct laser writing of three-dimensional photonic-crystal templates for telecommunications," *Nat. Mater.* **3**, 444–447 (2004).
17. Z. L. Zhang, A. S. Keys, T. Chen, and S. C. Glotzer, "Self-assembly of patchy particles into diamond structures through molecular mimicry," *Langmuir* **21**, 11547–11551 (2005).
18. V. N. Manoharan and D. J. Pine, "Building materials by packing spheres," *MRS Bull.* **29**, 91–95 (2004).
19. A. P. Hynninen, J. H. J. Thijssen, E. C. M. Vermolen, M. Dijkstra, and A. van Blaaderen, "Self-assembly route for photonic crystals with a bandgap in the visible region," *Nat. Mater.* **6**, 202–205 (2007).
20. S. Simeonov, U. Bass, and A. R. McGurn, "Photonic band structure of zinc blende type periodic dielectric media," *Physica B* **228**, 245–250 (1996).
21. H. S. Sözüer, J. W. Haus, and R. Inguva, "Photonic Bands - Convergence Problems with the Plane-Wave Method," *Phys. Rev. B* **45**, 13962–13972 (1992).
22. A. Moroz and C. Sommers, "Photonic band gaps of three-dimensional face-centred cubic lattices," *J. Phys.: Condens. Matter* **11**, 997–1008 (1999).
23. K. Edagawa, S. Kanoko, and M. Notomi, "Photonic amorphous diamond structure with a 3D photonic band gap," *Phys. Rev. Lett.* **100**, 013901 (2008).
24. R. Biswas, M. M. Sigalas, G. Subramania, and K. M. Ho, "Photonic band gaps in colloidal systems," *Phys. Rev. B* **57**, 3701–3705 (1998).
25. X. D. Wang, T. C. Leung, B. N. Harmon, and P. Carra, "Circular Magnetic-X-Ray Dichroism in the Heavy Rare-Earth-Metals," *Phys. Rev. B* **47**, 9087–9090 (1993).
26. A. Moroz, "Density-of-States Calculations and Multiple-Scattering Theory for Photons," *Phys. Rev. B* **51**, 2068–2081 (1995).
27. A. R. Williams and J. v.-W. Morgan, "Multiple scattering by non-muffin-tin potentials: general formulation," *J. Phys. C* **7**, 37–60 (1974).
28. W. H. Butler, A. Gonis, and X. G. Zhang, "Multiple-Scattering Theory for Space-Filling Cell Potentials," *Phys. Rev. B* **45**, 11527–11541 (1992).
29. W. H. Butler, A. Gonis, and X. G. Zhang, "Basis Functions for Arbitrary Cells in Multiple-Scattering Theory," *Phys. Rev. B* **48**, 2118–2130 (1993).
30. S. G. Johnson and J. D. Joannopoulos, "Block-iterative frequency-domain methods for Maxwell's equations in a planewave basis," *Opt. Express* **8**, 173–190 (2001).
31. "http://ab-initio.mit.edu/wiki/index.php/Main_Page,".
32. K. Busch and S. John, "Photonic band gap formation in certain self-organizing systems," *Phys. Rev. E* **58**, 3896–3908 (1998).
33. H. Míguez, F. Meseguer, C. López, A. Blanco, J. S. Moya, J. Requena, A. Mifsud, and V. Fornés, "Control of the photonic crystal properties of fcc-packed submicrometer SiO₂ spheres by sintering," *Adv. Mater.* **10**, 480–483 (1998).
34. Z. Y. Li and Z. Q. Zhang, "Fragility of photonic band gaps in inverse-opal photonic crystals," *Phys. Rev. B* **62**, 1516–1519 (2000).

1. Introduction

Photonic crystals are structures with a periodically varying dielectric constant, the spatial period being of the order of the wavelength of light. Similar to the way that electrons are influenced by the atomic lattice of a semiconductor, photons can be multiply scattered by the periodic structure of a photonic crystal and interfere destructively, resulting in ranges of frequencies that

cannot propagate in a certain direction, called photonic stop gaps. When propagation becomes impossible for all directions and polarizations within the photonic structure, the structure has a photonic band gap. Structures with an (almost) complete photonic band gap open the way for fundamental studies on, for example, inhibition of spontaneous emission [1, 2, 3, 4, 5] and they are interesting for the realization of photonic analogues of electronic circuits, including low-loss waveguides, optical diodes and transistors (for recent reviews see [6, 7, 8]).

Motivated by the interesting possible photonic applications and fundamental physical aspects, many studies have focused in the last two decades on designing three-dimensional photonic crystals with a photonic band gap. Until now, the most promising candidates for opening up a large band gap at relatively low refractive index contrasts are the diamond [9, 10, 11] and pyrochlore [12, 13] structures. Several methods for an experimental realization of the diamond and pyrochlore structures have already been proposed [13, 14, 15, 16, 17, 18, 19], including a recent method to fabricate both the diamond and the pyrochlore structure from the binary Laves structure MgCu_2 through self-organization [19]. In the MgCu_2 structure, the large (Mg) sphere component forms a diamond structure, while the small (Cu) sphere component forms a pyrochlore structure. Therefore, when the MgCu_2 structure is fabricated from spheres of different materials, one of the materials can be selectively removed, yielding the desired photonic colloidal crystal. This method is a promising route for the experimental fabrication of these colloidal structures and may even lead to a photonic band gap in the visible, because a photonic band gap opens up in diamond and pyrochlore for relatively low contrast, thus allowing a broader range of materials to be used. The other related Laves structures (MgZn_2 and MgNi_2) have free energies very close to that of MgCu_2 and are also composed of arrangements of small and large spheres in tetrahedrons.

The photonic properties of diamond structures of dielectric spheres have been thoroughly investigated using both plane-wave calculations [9, 10] and the Korringa-Kohn-Rostoker (KKR) method [11]. However, for the pyrochlore structure, only plane-wave calculations have been performed [12, 13], while it is known that there can be a discrepancy between the two methods [9, 11, 20, 21, 22]. Furthermore, previous photonic calculations on pyrochlore structures have focused on maximizing the photonic band gap, for example, by considering non-close-packed structures, focusing less on feasibility to realize these structures experimentally by self-organization. To expand our knowledge on the photonic properties of the crystal structures that can be realized by self-organization, related to the binary Laves structures, we present here plane-wave and KKR calculations for the photonic band diagrams of close-packed, dielectric Laves structures and their one-component constituent structures. We were interested in all constituent structures (not only diamond and pyrochlore) as they consist of tetrahedral arrangements of spheres and it has recently been shown that even an “amorphous” diamond photonic crystal structure, consisting of atoms with tetrahedral bonding symmetry, but no long-range order (like in a glass of silicon), has a large photonic band gap [23].

Infiltrating colloidal structures with a high-dielectric material yields inverted structures (with low-dielectric spheres in a high-dielectric background), which in some cases have a larger gap width than the direct structures (e.g. fcc [24, 22]). Therefore, also the inverted pyrochlore and diamond structures are considered. Comparing the results from both calculation methods for direct structures sheds new light on the convergence of band structure calculations of diamond related structures.

2. Band structure calculations

Photonic band structure diagrams were calculated up to band 10 for dielectric contrasts ranging from 2 to 20 using the photonic analogue of the Korringa-Kohn-Rostoker (KKR) method [11, 25, 26]. This method is optimized for crystals of spheres, but can be used for scatterers

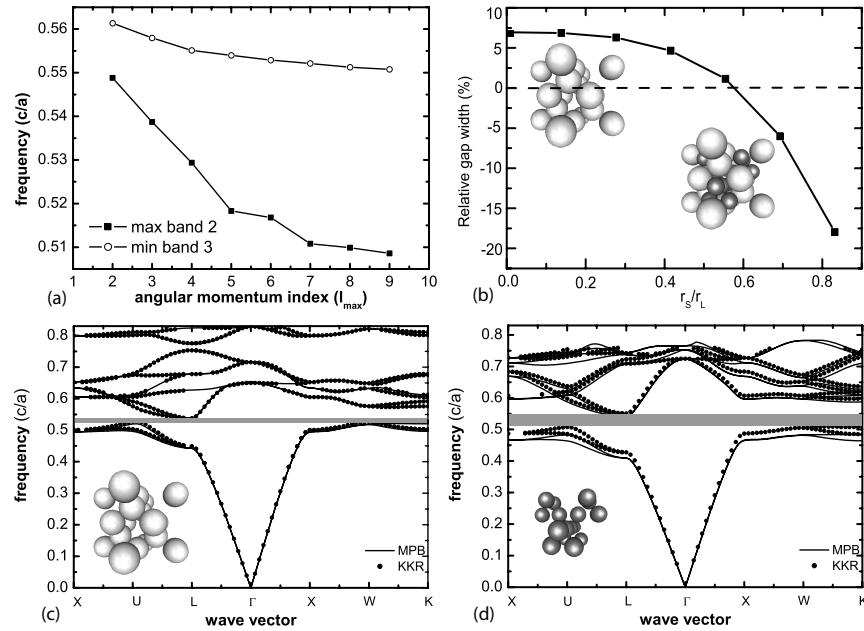


Fig. 1. (a) Convergence of the maximum frequency of band 2 and the minimum frequency of band 3 of the KKR band structure of the direct pyrochlore crystal of close-packed silicon spheres in air (dielectric contrast 12) with increasing values of l_{max} . (b) Relative gap width of various $MgCu_2$ structures. The large spheres are close-packed, the small sphere radius is varied. A size ratio of $r_S/r_L = 0$ corresponds to diamond, $r_S/r_L \approx 0.82$ corresponds to close-packed $MgCu_2$. All spheres consist of silicon ($\epsilon = 12$), the surrounding medium is air ($\epsilon = 1$). For negative relative gap widths, the maximum of the lower band is higher than the minimum of the higher band, therefore, the structure has no band gap. The line is a guide to the eye. (c-d) Band structure diagrams calculated by the plane-wave method (solid lines) and the KKR method (symbols) of (c) a direct diamond crystal and (d) a direct pyrochlore crystal, both of silicon spheres in air (dielectric contrast 12). Resolution 32 was used for the direct pyrochlore structure. Resolution 28 was used for the direct diamond structure, because we found that the lower branch in Fig. 3(a) converges faster, see Section 4.

of arbitrary shape [27, 28, 29]. Spherical harmonics were included up to angular momentum index $l_{max} = 9$. The convergence of the method for increasing l_{max} was checked (Fig. 1(a)). We compared our KKR results to plane-wave calculations, employing a unit cell, discretized by a grid of $32 \times 32 \times 32$ points, performed using the MIT Photonic Bands (MPB) software package [30]. This package computes fully-vectorial eigenmodes of Maxwell's equations with periodic boundary conditions by preconditioned conjugate-gradient minimization of the block Rayleigh quotient in a plane-wave basis [31]. For the calculations we presented here, we used MPB 1.4.2, modified to calculate the effective dielectric constant of Wigner-Seitz real-space unit cells instead of the parallelepiped unit cells spanned by the lattice vectors. We did not find any major differences between calculations that were performed with or without this patch, only absolute differences below 0.5%-point in the relative gap width for resolutions between 12 and 64 were found (where the resolution cubed equals the number of grid points).

We emphasize that the structures for which band diagrams have been calculated have not been optimized in any way. Optimization might be achieved for instance by using incomplete filling, which increases gaps for inverse fcc structures [32], or by slightly sintering the structures [33]. Both enhancement methods result in structures with overlapping spheres and are experimentally realizable. Although the KKR method can be used for scatterers of arbitrary shape [27, 28, 29], our implementation only allows for calculations of photonic band diagrams for muffin-tin scatterers, photonic band diagrams of the structures with overlapping spheres cannot be calculated with our code.

3. Results

For both the pyrochlore and the diamond structures, we have found band gaps between bands 2 and 3 and between bands 8 and 9 (Fig. 1(c) and 1(d)). We have focused on the band gap between bands 2 and 3, because this band gap is relatively large and it is more stable against disorder and defects [34]. Figure 2 shows the relative gap width of the photonic band gap between bands 2 and 3, as a function of the dielectric contrast, for both the direct and the inverse structures, at the maximum sphere packing fraction (of 34% for diamond and 37% for pyrochlore) calculated by using both the KKR-method and the MPB software. The relative gap width is defined as the ratio of the gap width and the midgap frequency. The inverse structures have a relatively narrow band gap, which opens up for dielectric contrasts higher than 10 and 12 for pyrochlore and diamond, respectively. KKR and MPB agree on the relative gap width within 0.5%-point for the inverse structures.

The direct structures possess large photonic band gaps for moderate dielectric contrasts. The two calculation methods agree on the midgap frequency and on the value of the dielectric contrast at which the gap opens, which is around a dielectric contrast of 5 for both the diamond and the pyrochlore structure. This is much lower than the required contrast for an inverse face-centered cubic (fcc) structure of 8.4 found by plane-wave calculations [24] or 8.1 found by calculations using the KKR method [22]. The large difference in the calculated relative gap width for higher dielectric contrasts in direct diamond and direct pyrochlore is discussed in Section 4.

Figure 2 also demonstrates the gap competition for direct structures as was reported earlier for the direct diamond structure [11]: the relative gap width between bands 2 and 3 increases with increasing dielectric contrast, but above a certain value, the relative gap width decreases again. It was found that the turnover point coincides with the opening of a second photonic band gap between bands 8 and 9. The decrease in relative gap width was not observed in plane wave calculations for direct pyrochlore structures within the dielectric contrast range considered here.

Using the MPB software, we did not find full band gaps for any of the binary Laves structures in the dielectric contrast range of 2 to 20. Neither did we find any significant gaps for the single

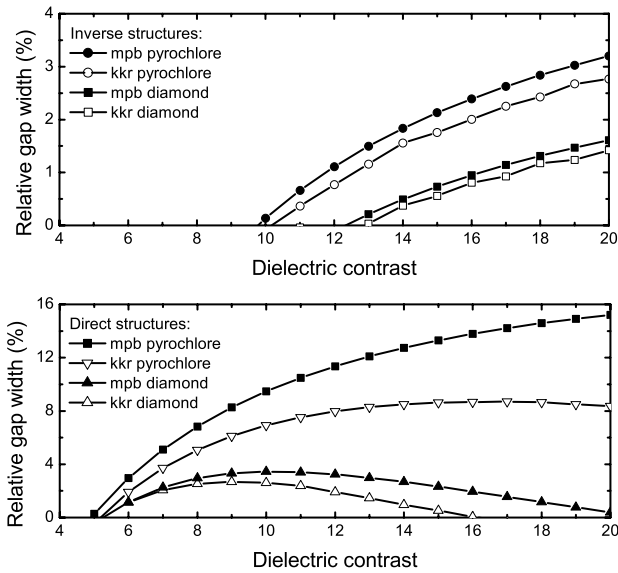


Fig. 2. The relative gap width of the photonic band gap between bands 2 and 3, as a function of the dielectric contrast, for the direct diamond and pyrochlore structures and their inverse structures at the maximum sphere packing fraction (of 34% and 37%, respectively), calculated by using both the KKR-method ($l_{max} = 9$) and MPB software (resolution 32 for the inverse structures and the direct pyrochlore structure and resolution 28 for the direct diamond structure, see Section 4). Note the difference in scale on the vertical axes. The solid lines are a guide to the eye.

small/large particle constituents of the MgZn_2 and MgNi_2 structures. We only found a 3.9% gap for the small sphere constituent of the MgNi_2 structure between bands 8 and 9, for a close packed structure of silicon spheres in air (dielectric contrast 12). The absence of a large band gap for the single-component constituent structures of MgZn_2 and MgNi_2 suggests that only a local tetrahedral arrangement is not enough for opening a band gap, as is suggested by Edagawa et al. [23]. Apparently also the combination of the global structure and the filling fraction of high-dielectric material plays a role.

To clarify the transition between the diamond structure, which has a band gap, and the binary MgCu_2 structure, which is without band gap, we looked at how the band gap of the diamond structure of large spheres closes upon insertion of the small spheres of the pyrochlore structure, thus forming MgCu_2 . We started with a close packed diamond structure of large spheres of silicon ($\epsilon=12$) in air ($\epsilon=1$) and increased the size of the small particles ($\epsilon=12$). The resulting graph is shown in Fig. 1(b). The band gap closes at a small-to-large size ratio of $r_S/r_L = 0.58$, while close-packed MgCu_2 is formed at a size ratio of $r_S/r_L = \sqrt{\frac{2}{3}} \approx 0.82$. The closing of the band gap can be ascribed to the increasing dielectric fraction together with a lack of connectivity of the dielectric phase, which makes it impossible to concentrate the field energy of successive bands in different dielectric phases and thus results in a featureless density of states (DOS) [10].

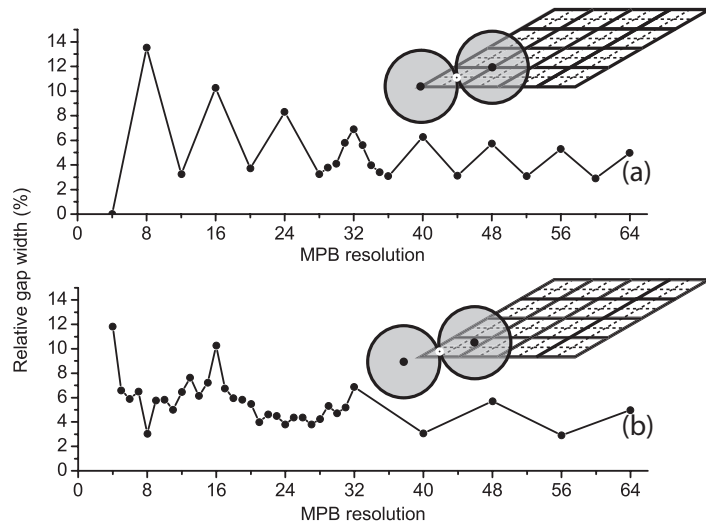


Fig. 3. Relative gap width between bands 2 and 3 of a close packed diamond structure of silicon spheres in air as a function of the chosen resolution in the MPB software with (a) the origin of coordinates on one of the spheres or (b) with the origin halfway between the center of the sphere and the contact point with the other sphere. The solid lines are a guide to the eye. The insets are 2D representations of the positions of the spheres and their contact point (white circle) with respect to the grid of the unit cell for resolution 4 (solid grid) and resolution 8 (solid+dashed grid).

4. Convergence of MPB band structure calculations

Comparing the KKR and plane-wave photonic band structure calculation methods in Fig. 2 shows that the KKR method systematically gives lower values for the relative gap width than the plane-wave method. Furthermore, the difference for the direct pyrochlore and diamond structures is much larger than the difference for the inverse structures. We examined the convergence of MPB and KKR more closely to find a possible cause of the discrepancy. Increasing the value of l_{max} in the KKR method shows that the results converge to one value for both the direct and the inverse structure, although the calculations for the direct structures converge slower than the calculations for the inverse structures. However, plotting the relative gap width versus the resolution in the MPB calculations (where (resolution)³ equals the number of plane waves included in the calculation) for a close-packed direct diamond structure of silicon spheres in air revealed an oscillating behavior, where the lower and the higher values slowly converge to one value (Fig. 3(a)). The oscillation period depends on the choice of the sphere coordinates with respect to the grid points. With one of the two spheres in the diamond unit cell centered on the grid origin, the oscillation period is 8, with high gap width values for resolutions that are multiples of 8 and low gap width values for resolutions that are multiples of 4, but not of 8. Similar oscillations, but with a period of 2, are found when the grid origin is on the contact point of the two spheres in the unit cell, i.e. when the structure has inversion symmetry.

A clue for this oscillation can be found in the coincidence of a sphere-contact point with an MPB grid point. When the origin is on the center of one of the spheres, the contact point is at coordinate $(\frac{1}{8}, \frac{1}{8}, \frac{1}{8})$ in the diamond unit cell. This contact point coincides with a grid point when the resolution is a multiple of 8, giving a high value for the relative gap width. The contact point is exactly in the middle of a grid box when the resolution is a multiple of 4, but not of 8,

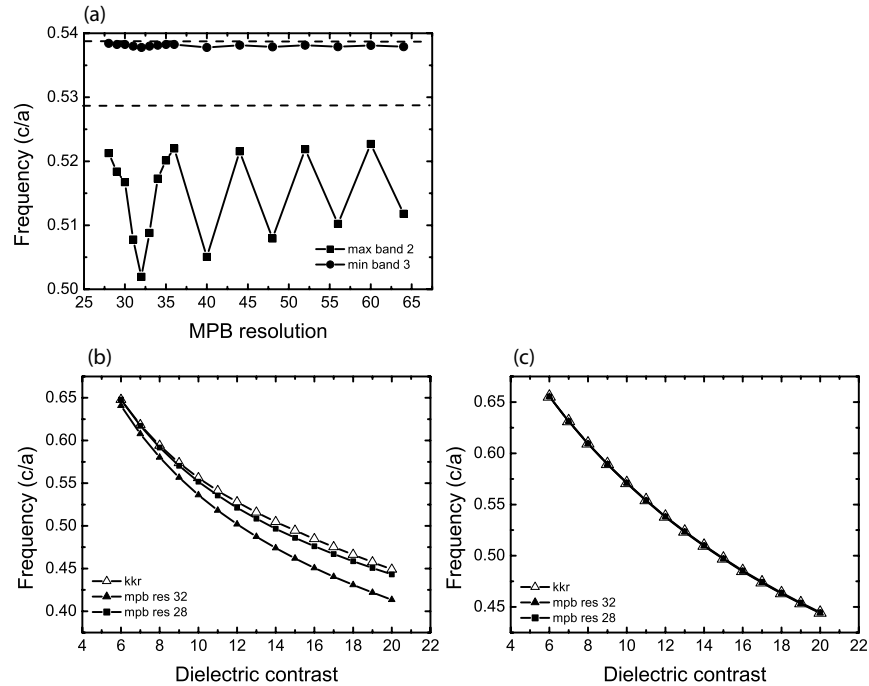


Fig. 4. Comparison of the maximum frequency for band 2 and the minimum frequency for band 3 for different resolutions. (a) Graph showing the calculated maximum frequency of band 2 and the calculated minimum frequency of band 3 as a function of the plane wave resolution for a configuration with one sphere in the origin. The straight dashed lines show the calculated values using the KKR method. The maximum frequency of band 2 (b) and the minimum frequency of band 3 (c) as a function of the dielectric contrast for the KKR method (open triangles) and for the plane wave method with resolution 32 (closed triangles).

giving a low value.

For an origin at a quarter of the line between the two spheres in the diamond unit cell (halfway between the center of one sphere and the contact point of the two spheres), the convergence-curve is shown in Fig.3(b). The clear local maximum and minimum, at resolution 8 and 16, respectively, can be explained in the same fashion: the contact point of the two spheres in this case is at $(\frac{1}{16}, \frac{1}{16}, \frac{1}{16})$. At a resolution of 8, this contact point is exactly in the middle of a grid box, yielding a low value for the relative gap width, while at a resolution of 16, the grid and the contact point coincide, giving a high value.

For the choice of origin equal to that for the graph in Fig. 3(a) (with the origin on one of the spheres), it was examined more closely from where the oscillations in the relative gap width originated. The maximum frequency of band 2 and the minimum frequency of band 3 have been plotted versus the MPB resolution in Fig. 4(a), finding oscillations for band 2 and almost no variation with resolution for band 3. The oscillation in the relative gap width thus comes from the maximum frequency value of band 2. This discrepancy in the value for band 2 is also reflected in the two last graphs in Fig. 4. In Fig. 4(b), the maximum frequency of band 2 is plotted against the dielectric contrast for both calculation methods. For increasing dielectric contrast, the difference between the values found by MPB and the values from KKR calculations increases significantly, while no significant difference is found for band 3 (Fig.

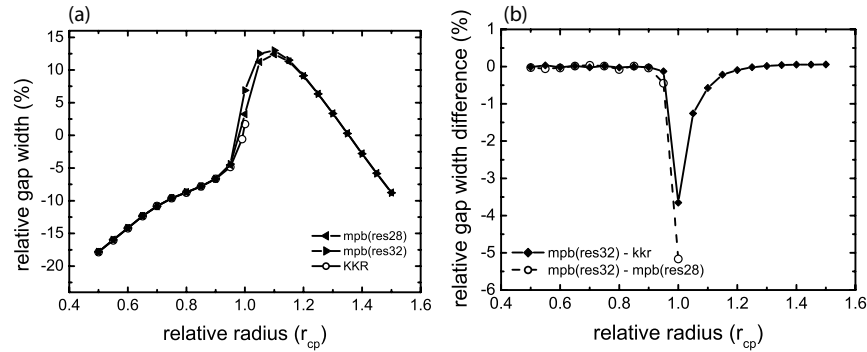


Fig. 5. Illustration of the deviation of the results of the different calculation methods and resolutions as a function of the relative radius near close packing for a configuration with one sphere in the origin. (a) The relative gap width as a function of the radius (expressed in r_{cp}). (b) Difference between the results of plane wave calculations at a resolution of 32 and the results of plane wave calculations at a resolution of 28 (solid squares) and between the results of plane wave calculations at a resolution of 32 and the results of the KKR method (open circles).

4(c)).

The importance of the contact point of the spheres becomes clear from the relation between the relative gap width and the relative radius of the spheres as plotted in Fig. 5(a). For clearly non-touching spheres (relative radius below 0.9), the calculations for both plane wave resolutions and the KKR calculations agree on the relative gap width within 0.1%-point. Also for overlapping spheres with a relative radius above 1.2 (for which KKR calculations are not available), the relative gap widths, calculated using resolution 28 and 32, agree within the same margin. However, for radii close to the close-packing radius (r_{cp}), the values start deviating from the KKR ones, especially for resolution 32. The deviation becomes more clear in Fig. 5(b), where the difference between the plane wave calculations at a resolution of 32 and the other two calculations is plotted. The three methods clearly disagree most around the close-packing radius, suggesting a connection of this deviation with the touching of the spheres.

We have performed additional MPB-calculations (not shown here) to investigate the dependence of the relative gap width on the coincidence of a contact point of two spheres and a grid point. These suggest that this dependence may be caused by the procedure with which MPB calculates the dielectric tensor for each grid point. However, the exact cause of the oscillations in the convergence would require the MPB source code to be adapted, which is outside the scope of this study. Unfortunately, we therefore cannot conclude at this moment whether the high or the low values which are calculated by the MPB program are closer to the actual value, we can only state that the lower values are closer to the values resulting from the calculations using the KKR method and that using both methods is recommended to check for consistency if numerical accuracy is important.

5. Conclusions

Band diagrams of various structures related to the binary Laves structures have been calculated using both plane-wave and KKR methods. We have not found significant band gaps for the binary Laves structures. Of the constituent single structures, only those of MgCu_2 , i.e. pyrochlore and diamond, give a photonic band gap that is interesting for photonic applications. Since a high filling fraction of dielectric material is disadvantageous for the gap width, the rela-

tive gap width found for diamond and pyrochlore was larger for the direct structures than for the inverse structures and it is also larger for pyrochlore than for diamond. Therefore, we conclude that the growth of a MgCu_2 colloidal crystal is a suitable starting point for the fabrication of a photonic crystal with a large photonic band gap. However, since no band gaps are found for the constituent structures of the other two Laves structures, selection of the desired Laves structure by epitaxial growth is critical [19].

KKR and MPB calculations agree upon the conclusions stated above and on the values of the dielectric contrast needed for a band gap to open. However, for high dielectric contrasts, the predicted relative gap widths start to disagree, due to a deviating value for the maximum frequency of band 2. These values from MPB calculations show an oscillation with resolution for certain configurations, where the sphere touching point coincides with a plane wave discretization grid point for alternating resolutions. The relation between the deviation and the touching of close-packed spheres was shown, together with the absence of the deviation for non-close-packed and overlapping spheres. In most other photonic structures, such as inverse fcc, this does not lead to severe convergence issues. In diamond, however, the gap width is a very sensitive function of the sphere radius near close-packing. This may lead to the observed dependence of the gap width on the position of the sphere centers on the grid. We therefore advise to always carefully check the convergence of plane wave calculations and to compare them to a different calculation method, especially for close-packed sphere systems with a large photonic band gap.

Acknowledgments

Authors JHJT and ECMV contributed equally to this work. The work of ECMV is supported by NanoNed, a nanotechnology program of the Dutch Ministry of Economic Affairs. JHJT's work is part of the research program of the *Stichting voor Fundamenteel Onderzoek der Materie (FOM)*, which is financially supported by the *Nederlandse Organisatie voor Wetenschappelijk Onderzoek (NWO)*.